Vibrational properties of rare-earth nitrides: Raman spectra and theory

S. Granville, C. Meyer, A. R. H. Preston, B. M. Ludbrook, B. J. Ruck, and H. J. Trodahl*
MacDiarmid Institute for Advanced Materials and Nanotechnology, School of Chemical and Physical Sciences, Victoria University of Wellington, P.O. Box 600, Wellington 6140, New Zealand

T. R. Paudel and W. R. L. Lambrecht
Department of Physics, Case Western Reserve University, Cleveland, Ohio 44106-7079, USA
(Received 13 November 2008; revised manuscript received 13 January 2009; published 12 February 2009)

Raman spectra are presented for the rare-earth nitrides SmN, GdN, DyN, ErN, and LuN measured with 633 and 514 nm excitation wavelengths and at temperatures above and below the Curie temperature. Frozen-phonon calculations are presented for the phonons at Γ, L, and X points in the same series of materials plus previously studied YbN using the full-potential linearized muffin-tin orbital method and the LSDA+U (local spin-density approximation+Hubbard U corrections). The method is found to be in good agreement with recent linear-response pseudopotential calculations for the closely related ScN. Comparison with ScN and Eu chalcogenides (EuS, EuO) allows us to conclude that the main spectral line seen in the RE-N is a disorder induced phonon density of states like spectrum heavily weighted by the LO(L) modes. Its second harmonic 2LO(L) is also observed. The increasing frequency trend with atomic number is related to the decreasing trend in lattice constant and hence increase in force constant rather than the mass of the rare-earth ion because this phonon mode is purely a N-vibrational mode. The disorder does not arise from the spin orientations because no changes are observed upon magnetic ordering but may arise from point defects and the size of the crystallites.

DOI: 10.1103/PhysRevB.79.054301 PACS number(s): 63.20.dk, 78.30.−j

I. INTRODUCTION

The rare-earth nitrides (RE-N) are a family of rocksalt compounds that have recently received renewed attention from both theory and experiment, driven largely by improved procedures in both. The theoretical situation has benefited from improved treatments of the partially filled 4f shell,[1–3] while the experiments have benefited from advances in thin-film growth and passivation procedures.[4–10] The attention has so far concentrated on their electronic and magnetic properties; it now appears that all RE-N that have been studied carefully are either narrow-gap semiconductors or semimetals, and that the moments sited in the RE 4f shell order ferromagnetically below a Curie temperature less than 70 K and are dependent on the RE element. In this paper we investigate their vibrational properties using a combined experimental and computational approach. Raman spectra are reported on thin films of SmN, GdN, DyN, ErN, and LuN. To the best of our knowledge there has been only one previous report of the phonons in rare-earth nitrides, namely, in YbN and Yb pnictides.[11,12] Although the rocksalt structure has no Raman active modes in first order, it is common to find significant scattering mediated by disorder or resonance.[13] Furthermore spin disorder above the Curie temperature, and the consequent orbital disorder, breaks the crystal symmetry and can lead to Raman scattering, as has been studied in the Eu chalcogenides.[14–16] It will be demonstrated below that the signal reported here is associated with disorder, most likely originating in the presence of N vacancies that are also known to dope the RE-Ns. We show that the electronic intermediate states involved in the Raman scattering couple most strongly to the N breathing mode, thus emphasizing the LO(L) modes.

II. EXPERIMENTAL METHODS

Detailed descriptions of the preparation of rare-earth nitride films and a range of characterization studies have been described in earlier publications,[4–7] and only a brief description will be given here. Most of the films in this report were grown by evaporation of the metals in the presence of 10^{-4} mbar of ultra pure nitrogen gas ("N_2-grown"), deposited on ambient-temperature substrates, which results in more-or-less strongly [111]-textured films on all of the substrates we have explored: Si covered by its natural oxide, sapphire, quartz, and silica glass. This growth mode is somewhat unusual for a NaCl crystal and will require further investigation. The propensity toward oxidation in moist air is controlled by capping the films, most successfully with nanocrystalline GaN. We have recently achieved epitaxial growth on yttria stabilized zirconia (YSZ) by pulsed laser deposition (PLD) in activated nitrogen onto substrates at elevated temperatures.[17] The films from both growth modes are stoichiometric within the 1%–2% accuracy of our measurements, and their oxygen concentration is of order 1%. They are grown to a thickness of typically 200 nm, with capping layers variously 50–200 nm thick. The films are indirect-gap semiconductors with direct optical gaps near 1 eV and carrier densities of order $0.3-1.0\times10^{19}$ cm^{-3} in N_2-grown films, and about 2 orders of magnitude larger in PLD films. The dominant dopant appears to be N vacancies. Here we report studies of SmN, GdN, DyN, ErN, and LuN. With the exception of LuN these are ferromagnetic at low temperature.

Ambient-temperature Raman spectra were collected with a Jobin-Yvon LabRam HR, using both the 633 nm (1.96 eV) line of a HeNe laser and the 514 nm (2.41 eV) Ar+line. The temperature dependence of the 514 nm-excited GdN spectrum through the Curie temperature was explored with the film mounted in a closed-cycle cryostat that is incompatible

with the LabRam configuration; for these measurements we used a Jobin-Yvon U1000 spectrometer fitted with a CCD detector. Both spectrometers require a notch filter to be fitted, which limits their response to Raman frequencies above 100–200 cm^{-1}. All measurements were performed in the quasibackscattering configuration. There was no evidence of any significant polarization-dependent effects. The spectra show features from the substrates and capping layer as well as the RE-N films, and in particular the signals from Si substrates were larger than the films' signal. Thus a correction has been applied to a few spectra shown below, subtracting the well-characterized Si spectrum. No corrections were applied for any other substrate or capping-layer signals.

III. COMPUTATIONAL METHODS

The underlying approach for our first-principles calculations is the density-functional theory in the local-density approximation. However, RE-N require special care to treat the open-shell strongly correlated $4f$ electrons. This is achieved here using the LSDA+U approach, originally introduced by Anisimov *et al.*[18,19] and applied to the RE-N by Larson *et al.*[2] We use the FP-LMTO method as implemented by Methfessel and van Schilfgaarde.[20] Forces are obtained in this method using a force theorem rather than by direct numerical differentiation.

To calculate phonons using the frozen-phonon approach, we apply small displacements of each of the atoms in each of the Cartesian directions. By evaluating the force components $F_{i\alpha}$ on each of the atoms in response to the small displacement $u_{j\beta}$ of the others we can calculate the force constants using numerical finite differences: $F_{i\alpha}=\Sigma_{j\beta}k_{i\alpha,j\beta}u_{j\beta}$. Diagonalizing the corresponding dynamical matrix, $D_{i\alpha,j\beta}=M_i^{-1/2}k_{i\alpha,j\beta}M_j^{-1/2}$ we obtain the phonon frequencies. Because of the periodicity, we obtain strictly speaking the Fourier transformed force constant at $\mathbf{q}=0$ only. However by doubling the cell either in the [001] or [111] direction, we also obtain the Brillouin zone folded modes at Γ. Thus we obtain the modes at L and X as well as those at Γ. By using larger cells, the modes at other $\mathbf{q}$ points could be obtained. However, by this approach we only obtain the TO modes at Γ. The long range electric field effect responsible for the LO-TO splitting is incompatible with the lattice periodicity and cannot be obtained in this manner.

The linear-response approach, which is based on density-functional perturbation theory,[21–23] on the other hand, readily solves the problem of the incommensurability of the phonon-mode wave at a general $\mathbf{q}$ with the primitive lattice cell. It does not require supercells and furthermore can incorporate long-range electric fields as present in LO response by means of Berry-phase calculations of the polarizability P_α and hence the Born dynamic effective charges $Z_{i\alpha,j\beta}=\partial P_\alpha/\partial\tau_{j\beta}$, which enter the theory of the LO-TO splitting. Here $\tau_{j\beta}$ is the position vector of the jth atom in the unit cell. This approach is thus far more powerful for phonon calculations. One can easily obtain the full phonon band structure and density of states (DOS). On the other hand, its implementation is currently mostly restricted to plane wave pseudopotential methods. In particular, we recently used the approach available in the open source code ABINIT (Ref. 24) for calculations of ScN and successfully identified various features in its Raman spectrum[25] with zone boundary modes dominating the DOS peaks.[26] ScN is a useful analog for the RE-N compounds because it also corresponds to column IIIb in the Periodic Table. In comparison with the REN, it avoids the complication of the $4f$ electrons and associated magnetism. The other main difference is of course the lighter mass of the Sc atom compared to the RE atoms.

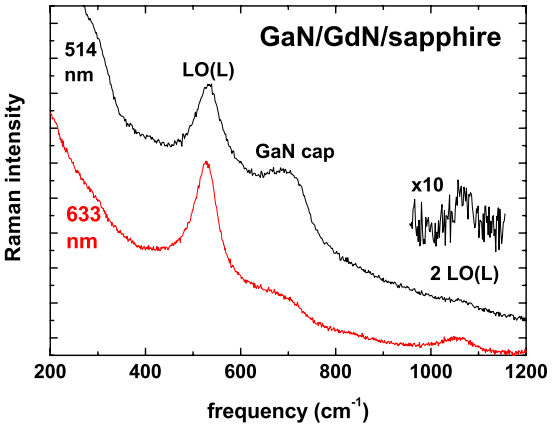

FIG. 1. (Color online) Raman spectra of GdN with 633 nm excitation (lower red) and 514 nm excitation (upper black).

The applicability of pseudopotential methods to RE elements however is doubtful. To test the FP-LMTO approach used here for the RE-N, we first show that it agrees well with the ABINIT results for ScN. The latter used a recently developed pseudopotential[27] for Sc which treats $3s$ and $3p$ electrons as valence states rather than as core states. Interestingly, we did not find this necessary in the FP-LMTO method, where we treat the $3s$ and $3p$ electrons as core orbitals. We also found that treating the $3p$ semicore states by means of local orbitals[28] did not improve the results. This indicates that the pseudizing of $3s$ and $3p$ orbitals is more severe than the core treatment in all electron approaches. Details of how the $3s$ $3p$ treatment in the pseudopotential approach affects the results for ScN are given in Ref. 26.

The FP-LMTO calculations for the RE-N were done with a large double basis set and including $5p$ orbitals as local orbitals, as in the calculations by Larson *et al.*[2] The Brillouin zone integration uses a well converged k-point set based on $6\times6\times6$ division of the reciprocal unit cell. We chose to evaluate the phonon frequencies at the experimental lattice constants rather than the theoretical equilibrium lattice constants, which were generally found to be overestimated by about 2%.[2]

IV. RESULTS

A. Experiment

Figure 1 compares the Raman data at 633 and 514 nm excitation for a GdN film deposited on sapphire and capped with GaN. In this case the GdN was sufficiently opaque to mask the weak sapphire Raman lines, so no correction was required. The same features appear under both excitations,

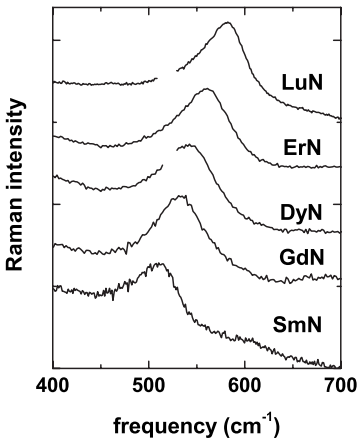

FIG. 2. Raman spectra of SmN, GdN, DyN, ErN, and LuN on an expanded scale to highlight the hardening across the RE series. The spectra for DyN and LuN show gaps where subtraction of the strong Si line was incomplete.

though at different relative intensities. Note first that the shoulder near 700 nm is from the GaN capping layer, as is the rise toward low frequencies.[29] The strongest line in the spectra, situated at 530 cm^{-1}, is a GdN vibration, which is seen also in second order at exactly twice that frequency. It is notable that the second harmonic appears stronger at 633 nm than at 514 nm, suggesting a resonant enhancement at the former. Note, however, that both the 514 and 633 nm excitations are above the 1.3 eV optical gap of GdN (Ref. 6) and no additional critical point transitions are expected in this range according to a recent calculation.[30] The second harmonic of the analogous line is found also in the other films reported here. Finally there is a shoulder near 350 cm^{-1} that is not attributable to the capping layer. Similar signals have been observed in most of the films, though often dominated, as here, by a low-frequency tail. Further exploration is required to establish the existence of that feature in the RE-N spectra with certainty.

The main-line spectra for all five nitrides are shown in Fig. 2, where a dependence on the ionic species is seen clearly. There is a continuous rise in the frequency with increasing atomic number due largely to a decreasing lattice constant as discussed below. Table I gives the frequencies of these features, as determined by a Lorentzian fit to the peaks. We also include here the literature value for YbN.[11]

The source of Raman activity in these rocksalt structures needs to be addressed. Note that Lu has a nonmagnetic filled

TABLE I. Raman main peak positions in RE-N.

Compound	ω (cm^{-1})
SmN	510
GdN	530
DyN	545
ErN	550
YbN	572[a]
LuN	582

[a]From Degiorgi *et al.* (Ref. 11).

TABLE II. Phonon frequencies in cm^{-1} for ScN with two computational approaches compared with experimental data.

	LMTO	ABINIT	
Mode	$3s3p$ core	$3s3p$ band	Expt.[a]
TO(Γ)	380	365	362
LO(Γ)		632	
TA(L)	245	234	242
LA(L)	499	464	
TO(L)	491	460	468
LO(L)	690	657	677
TA(X)	276	267	298
LA(X)	380	354	355
TO(X)	427	415	415
LO(X)	560	569	589

[a]From Travaglini *et al.* (Ref. 25) as discussed in Ref. 26.

$4f$ shell, so that the strength of the feature in LuN suggests that it is not rendered Raman active by spin disorder. The suggestion is corroborated by our temperature-dependent studies, which show no weakening of the feature as spin disorder is suppressed below the 70 K Curie temperature of GdN. Thus the signal is related to defects in the rocksalt structures, most likely associated with the same N vacancies that dope the films, as is further supported by an increased Raman activity in heavily doped PLD films.

B. Calculations

In Table II we show our results for ScN obtained with the present frozen-phonon FP-LMTO calculations compared with our previous linear-response ABINIT calculations. We can see that the LMTO frozen-phonon calculation gives results in fair agreement with the ABINIT linear-response calculation. More precisely, the LMTO calculation gives larger values by typically 5%–7%, except for the LO(X). We note however that the ABINIT calculation underestimates the experimental value for the main LO(L) peak by about 3%. The LMTO results overestimate the experimental value for the LO(L) by 2%. We can also see from the ABINIT results that the LO(Γ) mode is only slightly lower in frequency than the LO(L) mode.

Our results for the RE-N are shown in Table III. Compared with ScN, we may note that the gap between the acoustic branch and the optic branch is significantly larger. This is of course related to the heavier mass of the RE ions compared to ScN. In the latter the top of the LA branch at L even lies slightly higher than the TO modes at L and the acoustic and optic branch slightly overlap in the DOS. By comparison with ScN, we may also here expect that the TO branch has its minimum at the Γ point and its maximum along the $L-X$ line slightly above the TO(L) mode. The LO branch can be expected to have its maximum slightly above the LO(L) mode along $\Gamma-L$ and its minimum at Γ.

V. DISCUSSION

The Raman spectrum in the closely related material ScN, which also has the rocksalt structure, has strong similarities

TABLE III. Phonon frequencies of several RE-N in cm^{-1} calculated by frozen-phonon approach at the experimental lattice constant.

Mode	SmN	GdN	DyN	ErN	YbN	LuN
TO(Γ)	339	312	338	340	366	372
TA(L)	127	125	127	122	130	130
LA(L)	248	243	247	243	248	249
TO(L)	413	411	422	426	460	465
LO(L)	520	568	586	592	614	619
TA(X)	142	132	149	147	145	143
LA(X)	212	186	200	207	205	205
TO(X)	354	339	406	373	435	435
LO(X)	437	435	470	517	542	542

to those in the RE-N observed here. It was interpreted as a disorder induced first-order Raman spectrum by Travaglini *et al.*[25] This interpretation was further comfirmed and refined by a recent computational study of the phonon density of states.[26] It showed that the strongest Raman line is dominated by the LO(L) zone boundary phonons. Rather than just being proportional to the density of states, the zone boundary LO(L) modes are strongly enhanced because they have the most effective electron-phonon coupling to the electronic excitation. As in the present case 514 cm^{-1} excitation was used and is above the band gap in ScN as well. This means that we excite from mainly bonding to mainly antibonding electronic states. This can be expected to induce primarily fully symmetric breathing modes around the cation. The Raman spectrum is then weighted by a factor[14,15]

$$\left| \sum_{\alpha=1}^{3} \frac{e_\alpha(j,\mathbf{q})\sin(q_\alpha r_0)}{[\omega_j(\mathbf{q})]^{1/2}} \right|^2, \tag{1}$$

in which $\omega_j(\mathbf{q})$ is the frequencies of mode j at wave vector $\mathbf{q}$, $e_\alpha(j,\mathbf{q})$ is the normalized anion displacement in direction α for this mode, and r_0 the nearest-neighbor distance. As explained by Güntherodt *et al.*[15] this factor is minimum for the Γ point and maximum at the L points. In their study of the Eu chalcogenides, this dominant coupling to the breathing mode vibrations is related to the nature of the optical transition, which is a $f-d$ transition and is accompanied by zero energy spin wave excitations which help to conserve the crystal momentum. Here, this explanation is not applicable because the f states are much deeper and not related to the optical transition. However, as was also discussed for ScN,[26] the optical transition still corresponds to a transition from bonding (N-p-RE-d) to antibonding states and thus couples strongly to the breathing mode vibration affecting the RE-N bond lengths.

Assuming a similar interpretation is valid for the RE-N, we expect the main peak seen in all spectra to correspond to the LO(L) mode. The high frequency peak above 1000 cm^{-1} in all spectra appears to be an exact double of the low frequency peak and can thus be assigned to the 2LO(L) overtone.

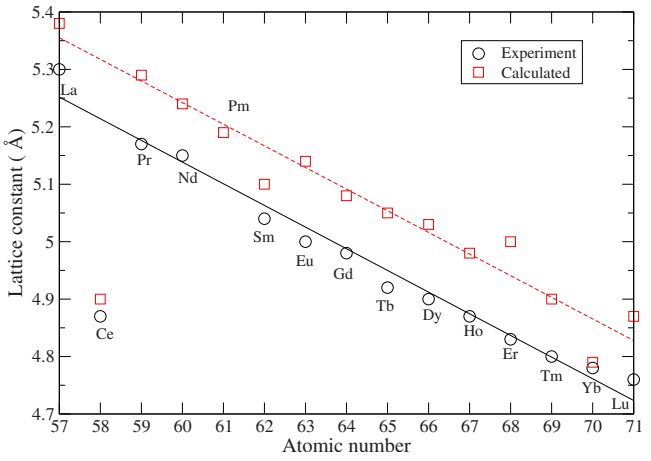

FIG. 3. (Color online) Lattice constants of rare-earth nitrides versus atomic number. The calculated results are from Larson *et al.* (Ref. 2).

Although the present data do not support a spin-disorder mechanism for the observed Raman activity it has not been possible to investigate fully the symptoms of that mechanism due to the polycrystalline nature of the films. For that purpose it would be required to determine the scattering symmetry expected from that mechanism, namely, the Γ_{15+} symmetry of the angular momentum operator appearing in the spin-orbit coupling Hamiltonian, if single crystalline samples become available. Still, the absence of any changes in the Raman scattering of GdN upon cooling below the Curie temperature and the observation of a similar Raman spectrum in LuN, which is not magnetic, already provide rather conclusive evidence that the spin-order mechanism cannot be the main origin of the Raman activity. To what extent the N vacancies and the polycrystalline nature of the films play a role will require further study. From the above discussion, it is also clear that the strong enhancement of the LO(L) mode is related to the exciting laser light being above the band gap, which is in some sense a resonance effect.

The LO(L) modes involve purely N atoms and hence should be independent of the mass of the RE. They should scale with the square root of the force constants or the strength of the RE-N bond. One may expect the latter to be roughly inversely proportional to the bond length squared. One then expects roughly an inverse proportionality with lattice constant. The latter decrease linearly across the rare-earth series as seen in Fig. 3. In this figure we also compare with the lattice constants obtained by Larson *et al.*[2] and see that these calculations show generally an overestimate by about 2% although the error is not quite uniform across the series. Also note that CeN does not follow the trend because Ce is tetravalent in CeN. This is the reason why we preferred here to use the experimental lattice constants. Thus, the interpretation of the main peak as LO(L) mode predicts a linear increase in the peak position with atomic number across the RE series. This is clearly observed in Fig. 4 for both the experimental and calculated frequencies. This fact by itself provides some evidence that the mode observed is a optic zone boundary mode. The same trend is predicted for the TO(L) and the TO(X), LO(X) modes. Our calculated fre-

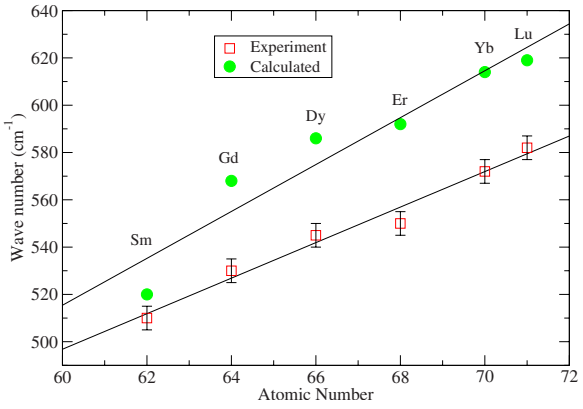

FIG. 4. (Color online) Experimental (main peak) and calculated LO(L) phonon frequencies versus atomic number. The lines are just linear interpolations as guide for the eyes. The experimental data include an error bar.

quencies are overestimated by about 6%. For acoustic modes at the zone boundary one would instead have obtained a dependence like $(m_R)^{-1/2}$ with m_R the rare-earth ion atomic mass and hence a decrease with increasing atomic number. For a zone center optic mode, the frequency would involve a factor $1/\sqrt{\mu}$ with μ the reduced mass $\mu = m_R m_N/(m_N+m_R)$. The latter however is varying only between 12.81 and 12.96 amu from Sm to Lu because the RE masses are all significantly higher than the N mass. So, it would be almost constant and the trend for a zone center optic mode would not differ very much from the zone boundary mode.

Finally, we note that the weak shoulder at 350 cm^{-1} in GdN matches reasonably well with our calculated TO(X) at 339 cm^{-1}. Interestingly, the TO(X) mode also coincides with one of the main peaks in ScN. For YbN, Degiorgi *et al.*[11,12] report a Raman spectrum that looks more like that of ScN in the sense that the lower frequency peak at 363 cm^{-1} is more prominent relative to the LO(L) peak at 572 cm^{-1} than in the RE-N observed here. They also extracted a value for the TO(Γ) mode at 274 cm^{-1} from the IR reflectivity. This is obtained by fitting a model to the plasmon coupled mode. They give a value of 500 cm^{-1} for the LO(Γ) from the zero of the model extracted dielectric function. Our calculations for YbN give a TO(Γ) at 366 cm^{-1} which is significantly higher. Also, the calculated TO(X) at 435 cm^{-1} is significantly higher than the low energy Raman peak at 363 cm^{-1}. This will require further study. On the computational side, we note that YbN has additional complications in that it does not follow the Hund's rule observed in the other RE-N.[2]

VI. CONCLUSIONS

A Raman study was presented of the RE-N vibrational properties. Raman spectra were measured for SmN, GdN, DyN, ErN, and LuN with 633 and 514 nm wavelength excitation. Zone center TO and zone boundary TA, LA, TO, and LO phonons at X and L were calculated for this same series and YbN, for which literature data are available.[11] Based on the similarity of the RE-N and ScN, which was recently studied by Paudel and Lambrecht,[26] the Raman spectra measured here for the RE-N are interpreted as disorder induced first-order Raman spectra, with main spectral weight at the LO(L) zone boundary phonons. The overtone of this is also observed in most spectra. The reason why the LO(L) is enhanced is explained in a similar fashion as for the Eu chalcogenides, namely, the strongest coupling of the electrons excited by the laser light happens to the breathing mode vibrations around the cation, because the laser light is above the band gap and hence excites the electrons from bonding to antibonding states, affecting the bond length to its neighbors. In contrast to the Eu chalcogenides, however, this is here a transition from mainly N-p-like to mainly RE-d-like, N-p-RE-d bonding and antibonding states, rather than an $f-d$ transition. The calculations overestimate the experimental values by about 4%–8%. Compared with the single crystal data on ScN and YbN, the TO(X) peaks seem somewhat suppressed in our samples but this may in part be because of the difficulties in distinguishing the RE-N signal from the substrate and/or capping layer signals in this energy range.

Consistent with the interpretation of the main peak as corresponding to LO(L) one finds that they scale linearly with the atomic number of the RE. This is because the mode is a pure N vibration mode and hence the mass of the RE does not play a role, but rather the frequency scales as the square root of the N-RE bond force constant which in turn scales approximately as 1/bond length squared. The lattice constants vary inversely proportional to the atomic number in the series. No significant changes in the spectra were observed under cooling below the Curie temperature, indicating that these spectra are not induced by spin-disorder but rather by other forms of disorder, most likely related to the presence of N vacancies.

ACKNOWLEDGMENTS

The MacDiarmid Institute is supported by a grant under the New Zealand Centres of Excellence program, and the present work has support from the New Zealand New Economy Research Fund. The work at CWRU was supported by the National Science Foundation World Materials Network Grant No. DMR-0710485. The calculations were performed at the Ohio Supercomputing Center.

*Also at Ceramics Laboratory, Swiss Federal Institute of Technology-EPFL, Lausanne 1015, Switzerland.

[1] C. M. Aerts, P. Strange, M. Horne, W. M. Temmerman, Z. Szotek, and A. Svane, Phys. Rev. B **69**, 045115 (2004).

[2] P. Larson, W. R. L. Lambrecht, A. Chantis, and M. van Schilfgaarde, Phys. Rev. B **75**, 045114 (2007).

[3] A. N. Chantis, M. van Schilfgaarde, and T. Kotani, Phys. Rev. B **76**, 165126 (2007).

[4] S. Granville *et al.*, Phys. Rev. B **73**, 235335 (2006).
[5] K. Khazen, H. J. von Bardeleben, J. L. Cantin, A. Bittar, S. Granville, H. J. Trodahl, and B. J. Ruck, Phys. Rev. B **74**, 245330 (2006).
[6] H. J. Trodahl, A. R. H. Preston, J. Zhong, B. J. Ruck, N. M. Strickland, C. Mitra, and W. R. L. Lambrecht, Phys. Rev. B **76**, 085211 (2007).
[7] A. R. H. Preston *et al.*, Phys. Rev. B **76**, 245120 (2007).
[8] F. Leuenberger, A. Parge, W. Felsch, K. Fauth, and M. Hessler, Phys. Rev. B **72**, 014427 (2005).
[9] F. Leuenberger, A. Parge, W. Felsch, F. Baudelet, C. Giorgetti, E. Dartyge, and F. Wilhelm, Phys. Rev. B **73**, 214430 (2006).
[10] J. W. Gerlach, J. Mennig, and B. Rauschenbach, Appl. Phys. Lett. **90**, 061919 (2007).
[11] L. Degiorgi, W. Bacsa, and P. Wachter, Phys. Rev. B **42**, 530 (1990).
[12] L. Degiorgi, S. Teraoka, G. Compagnini, and P. Wachter, Phys. Rev. B **47**, 5715 (1993).
[13] *Light Scattering in Solids, I*, edited by M. Cardona (Springer-Verlag, Berlin, 1975), Vol. 8.
[14] R. Merlin, R. Zeyher, and G. Güntherodt, Phys. Rev. Lett. **39**, 1215 (1977).
[15] G. Güntherodt, R. Merlin, and P. Grünberg, Phys. Rev. B **20**, 2834 (1979).
[16] R. Zeyher and W. Kress, Phys. Rev. B **20**, 2850 (1979).
[17] I. Farrell, B. Ludbrook, B. J. Ruck, A. R. H. Preston, and S. Durbin (unpublished).
[18] V. I. Anisimov, J. Zaanen, and O. K. Andersen, Phys. Rev. B **44**, 943 (1991).
[19] A. I. Liechtenstein, V. I. Anisimov, and J. Zaanen, Phys. Rev. B **52**, R5467 (1995).
[20] M. Methfessel, M. van Schilfgaarde, and R. A. Casali, in *Electronic Structure and Physical Properties of Solids. The Use of the LMTO Method*, edited by H. Dreyssé, Lecture Notes in Physics Vol. 535 (Springer-Verlag, Berlin, 2000), p. 114.
[21] S. Baroni, P. Giannozzi, and A. Testa, Phys. Rev. Lett. **58**, 1861 (1987).
[22] X. Gonze, Phys. Rev. B **55**, 10337 (1997).
[23] X. Gonze and C. Lee, Phys. Rev. B **55**, 10355 (1997).
[24] X. Gonze, J.-M. Beuken, R. Caracas, F. Detraux, M. Fuchs, G. M. Rignanese, L. Sindic, M. Verstraete, G. Zerah, and F. Jollet, Comput. Mater. Sci. **25**, 478 (2002); http://www.abinit.org
[25] G. Travaglini, F. Marabelli, R. Monnier, E. Kaldis, and P. Wachter, Phys. Rev. B **34**, 3876 (1986).
[26] T. R. Paudel and W. R. L. Lambrecht, Phys. Rev. B (to be published).
[27] C. Hartwigsen, S. Goedecker, and J. Hutter, Phys. Rev. B **58**, 3641 (1998).
[28] D. Singh, Phys. Rev. B **43**, 6388 (1991).
[29] H. J. Trodahl, F. Budde, B. J. Ruck, S. Granville, A. Koo, and A. Bittar, J. Appl. Phys. **97**, 084309 (2005).
[30] C. Mitra and W. R. L. Lambrecht, Phys. Rev. B **78**, 195203 (2008).